Phenolic Compound in Garlic (*Allium sativum*) and Black Garlic Potency as Antigout Using Molecular Docking Approach

Ayu Rahmania Lestari [a], Irmanida Batubara [a,b,*], Setyanto Tri Wahyudi [b,c], Auliya Ilmiawati [a,b]

[a] Department of Chemistry, Faculty of Mathematics and Natural Sciences, IPB University, Bogor, Indonesia
[b] Tropical Biopharmaca Research Center, IPB University, Bogor, Indonesia
[c] Department of Physics, Faculty of Mathematics and Natural Sciences, IPB University, Bogor, Indonesia

*Corresponding author: ime@apps.ipb.ac.id

Article Info

Abstract

Phenolics, including flavonoids, are bioactive components in garlic in relatively abundant amounts and are present 2–4 times more in black garlic. Both of these compounds are reported to have biological activity, with one of them acting as an antioxidant. However, its ability as an antigout is still not widely reported. Xanthine oxidase, adenine deaminase, guanine deaminase, purine nucleoside phosphorylase, and 5-Nucleotidase II are involved during the production of uric acid and causes gout. This study predicted the potential of the phenolic and flavonoid compounds in garlic and black garlic as antigout in inhibiting five target receptors through a molecular docking approach. Utilizing AutoDock Tools v.1.5.7 for receptor and ligand preparation, AutoDock Vina and AutoDock4 for molecular docking, and LigPlot⁺ and PyMOL for visualization. About 21 compounds from the phenolic and flavonoid groups were used as test ligands and 16 reference ligands (substrate and commercial). SwissADME predicted the pharmacokinetic parameters. The results showed that apigenin, morin, resveratrol, kaempferol, (+)-catechin, isorhamnetin, and (-)-epicatechin were predicted to have good interactions at each target receptor and had the potential to be developed as candidates for multi-target antigout. Based on the pharmacokinetic parameters, all these compounds had good scores in each, making them feasible to continue in vitro or in vivo trials.

1. Introduction

Garlic (*Allium sativum* L.) is a bulbous flowering plant widely used in culinary and cultivated in various countries in Asia, such as China, Japan, and Indonesia. Garlic bulbs are also reported to have antibacterial, antimicrobial, anti-inflammatory, and immunomodulatory properties due to their high sulfur compound content [1, 2]. In addition to sulfur compounds, phenolic compounds such as flavonoids are reported as natural antioxidants [3], suitable for treating heart disease and cancer, reducing the risk of chronic diseases, and preventing and treating atherosclerosis [4], are also available in relatively abundant quantities [5].

Black garlic is a garlic product that has been heated to high temperatures with controlled humidity for several days. In recent years, black garlic has emerged as a new product with different characteristics from garlic. Black garlic was first introduced in Japan and is gaining popularity in several countries such as China, South Korea, the US, and Europe because of its nutritional content and bioactive components better than garlic [6]. Several sensory properties change during the garlic-to-black garlic process, including a darker color due to an increase in melanoidin, a less intense taste and smell due to a decrease in sulfur compounds, and an increase in phenolic, flavonoids, and S-allyl cysteine (SAC) [7, 8]. Black garlic is reported to be good for preventing cardiovascular, cancer, obesity, and inflammation [6, 9, 10]. Black garlic has much higher antioxidant activity than garlic because it contains more phenolics, including flavonoids [10]. However, the ability of phenolic

compounds in garlic and black garlic as antigout has not been widely reported. Only quercetin in garlic has been reported to reduce blood uric acid levels [11]. Therefore, it is necessary to explore the ability of phenolic compounds, particularly flavonoids, in garlic and black garlic as antigout.

Gout is a condition in which the body synthesizes excessive amounts of uric acid. The synthesis of uric acid in our body is catalyzed by several enzymes, including xanthine oxidase (XDH) [12], adenine deaminase (ADA), guanine deaminase (GDA) [13], purine nucleoside phosphorylase (PNP) [14], and 5-nucleotidase II (NT5C2) [15]. Gout patients are treated clinically by taking allopurinol and febuxostat, which inhibit XDH activity and thus reduce uric acid production. However, both drugs have side effects such as liver and kidney toxicity [16]. As a result, gout patients frequently have comorbidities such as hypertension, diabetes, and hyperlipidemia [17].

The decrease in uric acid levels in the blood thus far is achieved by inhibiting a single enzyme, XDH [11, 18, 19]. However, single enzyme inhibition in lowering uric acid levels may be less effective. This study tried to inhibit all enzymes that play a role in uric acid biosynthesis using a molecular docking approach. This method is used because it can predict the binding conformation of ligands to the appropriate target binding site, which is essential in drug design and elucidating fundamental biochemical processes [20]. Therefore, this study aimed to predict the potential of compounds from the phenolic group, including flavonoids in garlic and black garlic as antigout, by inhibiting all target receptors using a molecular docking approach.

2. Methods

2.1. Tools, materials, and preparation of ligand and protein

The tools used in the research were Intel Core i7-8550U processor specifications laptop with 16384 MB RAM, and the software used was AutoDock Tools v.1.5.7 (https://ccsb.scripps.edu/mgltools/), AutoDock Vina (https://vina.scripps.edu/), AutoDock4 (https://AutoDock.scripps.edu/AutoDock4/), PyMOL (https://pymol.org/2/), and LigPlot+ v.2.2 (https://www.ebi.ac.uk/thornton-srv/software/LigPlus/). The materials used were the three-dimensional structure of enzyme XDH (PDB ID: 2E1Q), ADA (PDB ID: 3IAR), GDA (PDB ID: 4AQL), PNP (PDB ID: 1RSZ), NT5C2 (PDB ID: 2JC9) and the database contains 21 compounds from phenolic and flavonoid groups in garlic and black garlic as test ligands, and 16 reference ligands consisting of 11 substrates and 5 commercial ligands (Table 1 and 2). In addition, literature on the ligand was obtained from literature related to garlic and black garlic compounds.

The database used for molecular docking was taken from the Pubchem database catalog (https://pubchem.ncbi.nlm.nih.gov/). The ligand molecule was geometrically optimized using Orca2 software to resemble its natural state. The ligand was prepared using AutodockTools v.1.5.7 by first adding a hydrogen atom, detecting the root, and selecting the torque. The target protein molecules were taken from the

Protein Data Bank (https://www.rcsb.org/). The receptors and their natural ligands were separated and converted into PDB format using AutoDock Tools v.1.5.7. Water molecules and other heteroatom molecules were removed. Furthermore, adding polar hydrogen and a Kollman charge after checking for any missing atoms and then saving the file as *.pdbqt.

Table 1. Bioactive compounds on garlic and black garlic as test ligands

| No | Test ligands | Found in | | Ref. |
		Garlic	Black garlic	
1	(–)-Epigallocatechin gallate	✓	✓	[21]
2	(–)-Epicatechin	✓	✓	[21, 22]
3	(+)-Catechin	✓	✓	[21]
4	*p*-hydroxybenzoic acid	✓	✓	[10]
5	Apigenin	✓	✓	[22]
6	Caffeic acid	✓	✓	[21]
7	Chlorogenic acid	✓	✓	[21, 22]
8	Ferulic acid	✓	✓	[21]
9	Gallic acid	✓	✓	[21]
10	Isorhamnetin	✓	–	[23]
11	Kaempferol	✓	✓	[23]
12	Luteolin	✓	–	[23]
13	*m*-coumaric acid	✓	✓	[21]
14	Myricetin	✓	✓	[21]
15	Morin	✓	✓	[21]
16	*o*-coumaric acid	✓	✓	[21, 22]
17	*p*-coumaric acid	✓	✓	[21, 22]
18	Quercetin	✓	✓	[23]
19	Resveratrol	✓	✓	[21]
20	Vanillic acid	–	✓	[21]
21	Hesperidin	✓	✓	[22]

✓ = found, – = not found

Table 2. Reference ligands

Reference ligand			
Substrate	Ref.	Commercial	Ref.
Xanthine	[24]	Allopurinol	[25]
Hypoxanthine	[24]	Azepinomycin	[26]
Adenosine	[24]	Ulodesine	[27]
Guanine	[24]	Fludarabine	[28]
Guanosine	[24]	Xanthosine	[24]
Inosine	[24]	Adenosine monophosphate	[24]
Guanosine monophosphate	[24]	Xanthosine monophosphate	[24]
Inosine monophosphate	[24]	Erythro-9-(2-hydroxy-3-nonyl)adenine [EHNA]	[29]

2.2. Docking molecular simulation

Molecular docking of the receptor was conducted on the test and reference ligands. First, docking was done using AutoDock Vina. The receptor was redocking with co-crystal ligands before docking the test and reference ligands. This redocking aimed to obtain the coordinates of the receptor's active site. The structure of the protein and co-crystal ligands was made in the size of a grid box (search space) which covered the entire area of the receptor with sizes x, y, and z, as shown in Table 2 with 1.0 Å spacing. Grid box size data was stored in the *.config file format.

Then, co-crystal ligand binding to the receptor was done using AutoDock Vina based on the data in the config file. After the redocking was completed, docking

validation was performed between the co-crystal and docked ligand, where the validation parameter was the RMSD value ≤ 2 Å [30]. After being validated, the test and reference ligands were docked. The docking of the test and reference ligands used a binding site reference area based on the results of redocking. Docking results with AutoDock Vina were analyzed to obtain the highest binding energy. Five ligands with the highest binding energies were docked again using AutoDock4. The docking involved creating grid box sizes x = 60, y = 60, and z = 60 with 0.5 Å spacing. Grid box size data was stored in the *.gpf file format. The selected docking parameters were Genetic Algorithms (GA) run determined as 200 with the population size of 300, and the maximum number of evals was selected long (25 million). GA parameter data was stored in a *.dpf file format. Analysis of docking results in the form of Gibbs free energy and amino acid residue interactions were visualized using LigPlot+ 2.2 and PyMOL.

2.3. Screening of bioactive compounds as drug candidates

All compounds targeted by drug candidates were subjected to Lipinski's rule of five testing and ADMET (absorption, distribution, metabolism, excretion, and toxicity) testing through the ADMETsar website (http://www.swissadme.ch/).

3. Results and Discussion

3.1. Molecular docking simulation

Before docking, the docking method must be validated using AutoDock Vina software by redocking the co-crystal ligand to each receptor (Figure 1). However, as the xanthine oxidase receptor has no co-crystal ligand, a grid box was created by employing all of the amino acid active sites in the xanthine oxidase protein. The grid used in molecular docking can be seen in Table 3. The validation parameter was based on the RMSD value, which indicated the level of deviation of the docking ligand position against the co-crystal ligand. The smaller the RMSD value, the smaller the deviation between docking ligand positions and co-crystal ligands, and this position is considered to be the best. The RMSD value is said to be valid if ≤ 2 Å [30], and if it is in the range of 2−3 Å, the validation results are still acceptable [31].

The redocking of each receptor had an RMSD value of ≤ 2 Å. This value is acceptable, and the docking process is valid, so the grid box size and position for each receptor can be used for docking with the test ligand [32]. However, the xanthine oxidase protein does not have an RMSD value because the protein does not have a co-crystal ligand, so the docking method cannot be validated.

Table 3. Size of the redocking grid box

Receptor	Size (x, y, z) and center (x, y, z)	RMSD (Å)
Xanthine oxidase (XDH)	Size (24, 24, 24) Center (31.177, 22.319, 149.462)	n.a
Adenine deaminase (ADA)	Size (20, 20, 20) Center (6.361, −3.504, 0.741)	1.509
Guanine deaminase (GDA)	Size (16, 16, 16) Center (5.159, −26.598, 1.557)	1.767
Purine nucleoside phosphorylase (PNP)	Size (16, 16, 16) Center (2.247, 18.992, 25.392)	1.191
5-Nucleotidase II-1497 (NT5C2-1497)	Size (12, 12, 12) Center (−2.566, 18.342, 58.224)	0.778
5-Nucleotidase II-1498 (NT5C2-1498)	Size (13, 13, 13) Center (−22.736, 32.601, 49.929)	2.128

n.a = not available

Molecular docking is an *in silico* method to observe the best interactions between protein−ligand complexes. Molecular docking simulations in this study were performed employing AutoDock Vina software between XDH, ADA, GDA, PNP, and NT5C2 proteins with 21 test and 16 reference ligands consisting of 11 substrates and 5 commercial compounds for each target protein (Table 1 and 2). The XDH, ADA, GDA, PNP, and NT5C2 were used as target receptors because these five enzymes were directly involved in uric acid biosynthesis [24]. Figure 2 shows the mechanism of uric acid formation catalyzed by these five enzymes.
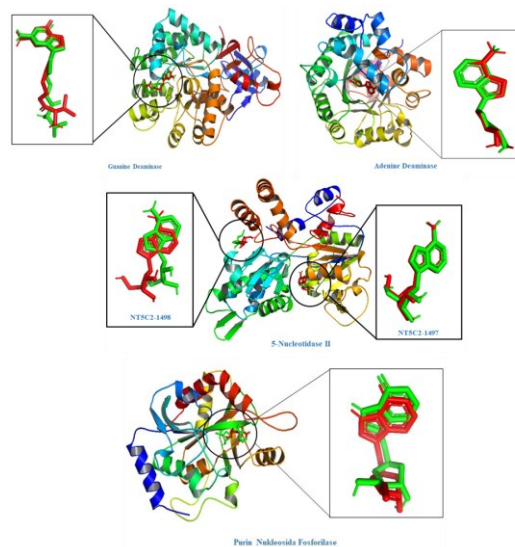

Figure 1. 3D visualization of the validation results of the docking method (notes: green = ligands contained in the protein structure (co-crystal ligand), red = redocking ligand, NT5C2-1497 and NT5C2-1498 = position of effector site 1 and effector 2 of protein 5-Nukleotidase II)
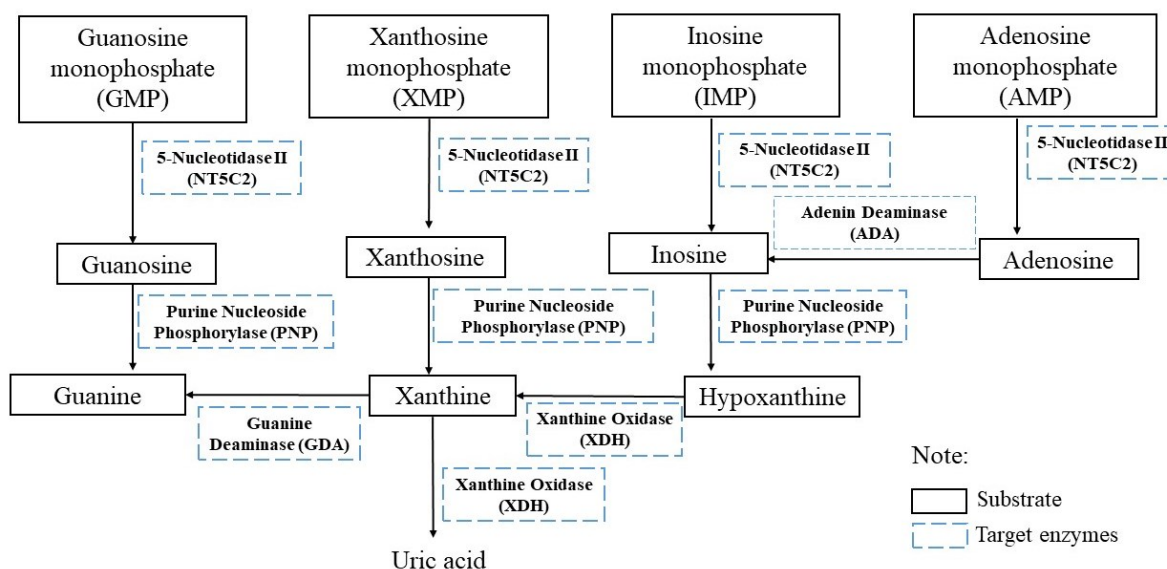
Figure 2. Uric acid biosynthesis mechanism

The Gibbs free energy, or the binding affinity of the ligand to the acceptor, is considered a determining factor in the stability of a ligand-protein complex [33]. The more negative the Gibbs free energy value or the binding affinity of the ligand to the receptor, the stronger the binding of the ligand to the target receptor, which causes the ligand to be better at inhibiting the target receptor [33]. The results of the docking simulation using the virtual screening method resulted in different energy affinities at each target receptor are tabulated in Table 4.

Based on the molecular docking results (Table 4), the energy affinity values of the test ligands ranged from −9.30 to −2.70 kcal/mol. The highest energy affinity values of −9.30 kcal/mol belonged to (−)-epicatechin and luteolin compounds when docked to the xanthine oxidase (XDH) receptor. Apigenin, luteolin, myricetin, quercetin, and isorhamnetin are compounds that bind strongly to all target receptors. The value of its energy affinity is more negative than commercial and substrates at each target receptor. The same thing happened to (−)-epicatechin, (+)-catechin, kaempferol, and morin which were bound to five different receptors, as shown in Table 3. (−)- Epigallocatechin was the only compound that could bind to four receptors, namely XDH, GDA, PNP, and NT5C2-1498.

Furthermore, caffeic acid binds to XDH, GDA, and NT5C2-1497 receptors, whereas chlorogenic acid binds to XDH, ADA, and GDA receptors. Ferulic acid, p-coumaric acid, and resveratrol are attached to the same two target receptors, XDH and GDA. Finally, m-coumaric acid, o-coumaric acid, and vanillic acid each bind to a single receptor, with m-coumaric acid and o-coumaric acid binding to the XDH receptor. In contrast, vanillic acid binds to the GDA receptor.

Based on molecular docking results of the 21 tested ligands, only p-hydroxybenzoic acid and gallic acid did not exhibit excellent binding affinities for all target receptors. In comparison, 19 other ligands are suspected as potential candidates for multi-target antigout because 19 compounds had good binding when compared to commercial and substrates at several different receptors based on the binding affinity value. The 19 compounds are highlighted in red (Table 4). This study's results differ from those previously reported, in which the test ligand compounds from the flavonoid group in garlic were said to only inhibit one target, specifically XDH [11].

A total of 19 test ligands from the docking were ranked, and 5 test ligands were taken from each receptor with the most negative energy affinity value compared to the reference ligands (substrate and commercial). The 5 test ligands with the most negative energy affinity values are highlighted in green (Table 4). The test ligands were docked again using the AutoDock4 method. The results of the docking are shown in Table 5. The purpose of docking with AutoDock4 was to compare the results of calculations based on scoring function differences of AutoDock4 with AutoDock Vina.

Based on Table 5, it can be seen that there is a difference in the energy affinity value of the docking results from AutoDock Vina and AutoDock4; this is due to the scoring function between the two methods. The scoring function in AutoDock4 is semi-empirical, involving Coulomb potential, Lennard-Jones potential, system desolvation, and conformational entropy. In contrast, the AutoDock Vina scoring function is empirical, consisting of Gaussian steric, hydrogen, hydrophobic, and covalent bonds [34]. AutoDock vina has the advantage of docking more quickly and accurately predicting the binding pose than AutoDock4. Nonetheless, AutoDock4 provides good accuracy and precision regarding energy affinity values correlated with experiments [34].

Table 4. Energy affinity of the test ligand docking with the target receptor

Ligand	Energy affinity (kcal/mol)					
	XDH	ADA	GDA	PNP	NT5C2-1497	NT5C2-1498
(−)-Epigallocatechin gallate	−8.30 ± 1,34	−6.27 ± 0,40	−6.97 ± 0,58	−8.50 ± 0,00	−3.83 ± 1,99	−5.73 ± 0,09
(−)-Epicatechin	−9.30 ± 0,05	−7.50 ± 0,00	−6.73 ± 0,05	−8.20 ± 0,00	−5.07 ± 0,25	−5.60 ± 0,00
(+)-Catechin	−8.87 ± 0,05	−8.10 ± 0,00	−6.97 ± 0,38	−8.50 ± 0,00	−5.37 ± 0,12	−5.37 ± 0,05
p-hydroxybenzoic acid	−6.10 ± 0,00	−5.90 ± 0,00	−6.17 ± 0,05	−5.50 ± 0,00	−4.10 ± 0,24	−3.87 ± 0,09
Apigenin	−8.90 ± 0,00	−7.60 ± 0,00	−7.87 ± 0,31	−8.70 ± 0,00	−5.23 ± 0,48	−5.60 ± 0,00
Caffeic acid	−6.80 ± 0,00	−6.80 ± 0,00	−6.67 ± 0,05	−6.50 ± 0,00	−4.83 ± 0,09	−4.50 ± 0,00
Chlorogenic acid	−8.90 ± 0,00	−7.77 ± 0,05	−9.00 ± 0,00	−8.10 ± 0,00	−3.77 ± 1.46	−5.33 ± 0,24
Ferulic acid	−7.03 ± 0,00	−6.40 ± 0,00	−6.80 ± 0,28	−6.40 ± 0,00	−4.77 ± 0,05	−4.53 ± 0,05
Gallic acid	−6.10 ± 0,05	−6.20 ± 0,00	−6.40 ± 0,00	−5.80 ± 0,00	−4.27 ± 0,21	−4.17 ± 0,05
Isorhamnetin	−8.17 ± 0,05	−7.90 ± 0,00	−6.90 ± 0,16	−8.40 ± 0,05	−5.33 ± 0,31	−5.60 ± 0,00
Kaempferol	−8.40 ± 0,00	−7.73 ± 0,05	−7.57 ± 0,33	−8.57 ± 0,05	−5.23 ± 0,42	−5.37 ± 0,05
Luteolin	−9.30 ± 0,00	−7.70 ± 0,00	−7.53 ± 0,19	−9.03 ± 0,09	−5.40 ± 0,37	−5.97 ± 0,05
m-coumaric acid	−6.87 ± 0,00	−6.93 ± 0,05	−6.40 ± 0,00	−6.00 ± 0,00	−4.80 ± 0,08	−4.53 ± 0,05
Myricetin	−8.50 ± 0,00	−7.40 ± 0,00	−6.97 ± 0,26	−9.20 ± 0,00	−4.97 ± 0,58	−5.67 ± 0,17
Morin	−8.60 ± 0,00	−7.30 ± 0,00	−6.90 ± 0,33	−8.67 ± 0,05	−5.17 ± 0,45	−5.33 ± 0,05
o-coumaric acid	−6.67 ± 0,05	−6.37 ± 0,05	−6.07 ± 0,05	−6.10 ± 0,00	−4.67 ± 0,05	−4.53 ± 0,05
p-coumaric acid	−6.63 ± 0,14	−6.33 ± 0,05	−6.70 ± 0,00	−6.10 ± 0,00	−4.47 ± 0,26	−4.10 ± 0,00
Quercetin	−8.40 ± 0,05	−7.70 ± 0,00	−7.03 ± 0,40	−9.00 ±0,00	−5.30 ± 0,49	−5.60 ± 0,00
Resveratrol	−8.20 ± 0,09	−7.13 ± 0,05	−7.87 ± 0,05	−7.50 ± 0,05	−4.80 ± 0,36	−5.03 ± 0,09
Vanillic acid	−4.2 ± 0,09	−5.70 ± 0,14	−6.50 ± 0,00	−5.80 ± 0,00	−4.23 ± 0,17	−4.23 ± 0,12
Hesperidin	−7.30 ± 0,00	−7.47 ± 0,25	−5.80 ± 0,78	−8.27 ± 0,75	−2.70 ± 0,00	−4.70 ± 0,73
Allopurinol (commercial)	−6.60 ± 0,00					
Xanthine (substrate)	−6.40 ± 0,00					
Hypoxanthine (substrate)	−6.23 ± 0,05					
Erythro-9-(2-hydroxy-3-nonyl)adenin [EHNA] (commercial)		−7.13 ± 0,05				
Adenosine (substrate)		−7.00 ± 0,00				
Azepinomycin (commercial)			−6.40 ± 0,00			
Guanine (substrate)			−6.00 ± 0,00			
Ulodesine (commercial)				−8.30 ± 0,00		
Guanosine (substrate)				−8.27 ± 0,05		
Inosine (substrate)				−7.83 ± 0,05		
Xanthosine (substrate)				−7.80 ± 0,00		
Fludarabine (commercial)					−4.80 ± 0,08	−5.23 ± 0,05
Adenosine monophosphate (substrate)					−4.73 ± 0,46	−5.40 ± 0,08
Guanosine monophosphate (substrate)					−3.87 ± 0,87	−5.43 ± 0,12
Inosine monophosphate (substrate)					−4.03 ± 1,39	−5.47 ± 0,26
Xanthosine monophosphate (substrate)					−3.33 ± 2,00	−4.70 ± 0,22

The binding affinity value of the test ligand is more nagative than commercial and substrate (highlight pink), test ligands for docking with Autodock4 (highlight green)

Table 5. Comparison of the energy affinity values of docking test ligands using AutoDock Vina and AutoDock4

Receptors	ligands	Energy affinity (kcal/mol)	
		AutoDock Vina	AutoDock4
Xanthine Oxidase	Allopurinol (commercial)	−6.60	−5.00
	Hypoxanthine (substrate)	−6.23	−5.00
	Xanthine (substrate)	−6.40	−5.29
	(−)-Epicatechin	−9.30	−8.16
	Luteolin	−9.30	−7.87
	Apigenin	−8.90	−8.28
	Chlorogenic acid	−8.90	−7.87
	(+)-Catechin	−8.87	−8.05
Purine Nucleoside fosforilase	Ulodosine (commercial)	−8.30	−6.24
	Guanosine (substrate)	−8.27	−7.60
	Inosine (substrate)	−7.83	−5.05
	Xanthosine (substrate)	−7.80	−6.13
	Myricetin	−9.20	−7.25
	Luteolin	−9.03	−7.56
	Quercetin	−9.00	−7.08
	Apigenin	−9.70	−7.61
	Morin	−8.67	−6.85
Guanine Deaminase	Azepinomycin (commercial)	−6.40	−5.39
	Guanine (substrate)	−6.00	−5.85
	Chlorogenic acid	−9.00	−6.45
	Apigenin	−7.87	−6.20
	Resveratol	−7.87	−6.27
	Kaempferol	−7.57	−5.87
	Luteolin	−7.53	−6.76
Adenine Deaminase	9-(2-hydroxy-3-nonyl)adenine [EHNA] (commercial)	−7.13	−5.65
	Adenosine (substrate)	−7.00	−5.75
	(+)-Catechin	−8.10	−7.73
	Isorhamnetin	−7.90	−7.09
	Chlorogenic acid	−7.77	−5.86
	Kaempferol	−7.73	−6.71
	Luteolin	−7.70	−7.34
5-Nucleotidase II 1497	Fludarabine (commercial)	−4.80	−4.25
	Adenosine monophosphate (substrate)	−4.73	−5.82
	Guanosine monophosphate (substrate)	−3.87	−5.44
	Inosine monophosphate (substrate)	−4.03	−4.76
	Xanthosine monophosphate (substrate)	−3.33	−4.48
	Luteolin	−5.40	−5.99
	(+)-Catechin	−5.37	−5.32
	Isorhamnetin	−5.33	−5.41
	Quercetin	−5.30	−5.69
	Apigenin	−5.23	−6.94
5-Nucleotidase II 1498	Fludarabine (commercial)	−5.23	−4.74
	Adenosine monophosphate (substrate)	−5.40	−5.18
	Guanosine monophosphate (substrate)	−5.43	−3.83
	Inosine monophosphate (substrate)	−5.47	−4.66
	Xanthosine monophosphate (substrate)	−4.70	−4.74
	Luteolin	−5.97	−6.11
	(−)Epigallocatechin gallate	−5.73	−6.10
	Myricetin	−5.67	−5.48
	(−)-Epicatechin	−5.60	−6.24
	Apigenin	−5.60	−6.09

3.2. Screening of bioactive compounds as drug candidates

For their pharmacological properties, the Lipinski test analyzed 12 ligands resulting from docking with AutoDock4 (Table 5). The Lipinski test aimed to determine the permeability and ability of the test ligand to be absorbed orally [35]. The rules required to abide by the Lipinski test are molecular weight < 500 Da, octanol/water partition coefficient (AlogP) < 5, number of hydrogen bond donors (HBD) < 5, and number of hydrogen bond acceptors (HBA) < 10 [36]. Lipinski's rule has a tolerance limit that is allowed to violate one rule

[35]. Allopurinol, ulodesine, azepinomycin, 9-(2-hydroxy-3-nonyl)adenine [EHNA], and fludarabine are commercial drugs that have been widely circulated and used to treat gout and passed the Lipinski test. This result is consistent with the finding tabulated in Table 6, which shows that the five commercial ligands did not violate the Lipinski test. Based on Table 6, the (−)-epigallocatechin gallate has exceeded the tolerance limit of the Lipinski test; namely, the number of hydrogen bond donors is eight, and the number of hydrogen bond acceptors is 11. Therefore, the compound (−)-epigallocatechin has poor

permeability and is unsuitable for oral use. Meanwhile, the other test ligands passed the Lipinski test.

The test was continued with the ADMET Test to determine ADMET (Absorption, Distribution, Metabolism, Excretion, and Toxicity) so that the pharmacology and pharmacokinetics of these compounds were known using the webserver http://www.swissadme.ch/ [37]. Five important ADMET indicators are bioavailability, Human Intestinal Absorption (HIA), AMES mutagenesis, carcinogenicity, and LD_{50} [38]. Bioavailability describes the ability of a drug to enter the systemic circulation, which ultimately accesses the active site. Meanwhile, absorption in the human gut, denoted as human intestinal absorption (HIA), is the ability of a drug to be absorbed into the intestine and digestive system. The next indicator is AMES Mutagenesis, which is the ability of drugs to cause mutations in test bacteria that can provide information related to the toxicity of compounds.

On the other hand, carcinogenicity indicates the potential of a compound to cause cancer. Positive and negative signs indicate whether or not they can occur [38]. The last indicator is LD_{50} which refers to the maximum dose in milligrams per kilogram of test animal weight that can cause death in test animals. Table 6 shows that allopurinol, azepinomycin, EHNA, fludarabine, and ulodesine as control compounds had good ADMET indicators. Based on the ADMET parameters (Table 6), almost all test compounds had good scores in each parameter, except for the Chlorogenic acid and (−)-epigallocatechin gallate had a low score on the bioavailability parameter (<0.55). Myricetin, luteolin, and quercetin had poor scores on carcinogenicity and AMES

mutagenesis parameters, so the five compounds are unsuitable to be recommended as antigout candidates. Finally, seven compounds were found that were suspected to be the best antigout candidates because they had good Lipinski and ADMET parameters. The selection of seven compounds as test ligands is schematically illustrated in the virtual screening protocol, as shown in Figure 3.
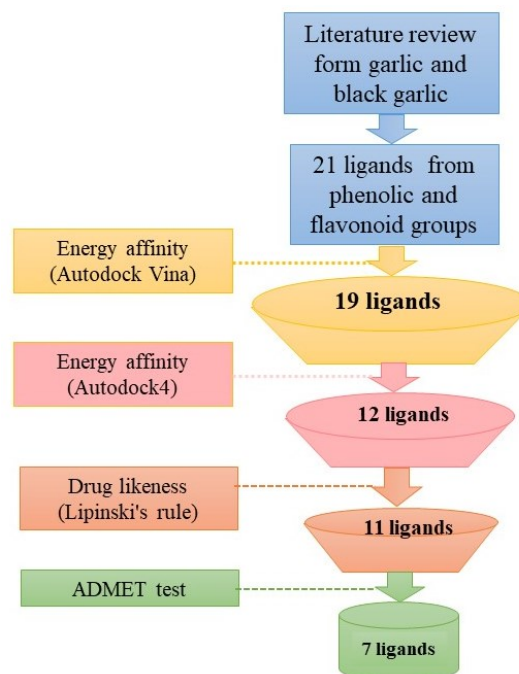

Figure 3. Compound virtual screening workflow as the antigout candidate

Table 6. Lipinski's rule and ADMET Test for the test and commercial ligands

Ligand	Lipinski's rule				ADMET Parameters				
	MW[a] (< 500 g mol^{-1})	LogP[b] (< 5)	HBD[c] (< 5)	HBA[d] (< 10)	Bioavailability (score)	Human Intestinal Absorption (HIA)	AMES Mutagenesis	Carcinogenicity	LD_{50} (mg/kg) (Predicted Toxicity Class)
Ulodesine	264.28	-0.797	4	6	GB (0.55)	HIA (+)	AMES (−)	NC	1000 (IV)
Azepinomycin	168.16	-1.116	4	5	GB (0.55)	HIA (+)	AMES (−)	NC	2032 (V)
Erythro-9-(2-hydroxy-3-nonyl)adenine [EHNA]	277.37	2.3	3	5	GB (0.55)	HIA (+)	AMES (−)	NC	450 (IV)
Fludarabine	285.24	-2.84	4	9	GB (0.55)	HIA (+)	AMES (−)	NC	13 (II)
Allopurinol	136	-0.187	2	4	GB (0.55)	HIA (+)	AMES (−)	NC	1000 (IV)
Myricetin	318.24	1.08	6	8	GB (0.55)	HIA (+)	AMES (+)	C	159 (III)
Luteolin	286.24	1.86	4	6	GB (0.55)	HIA (+)	AMES (+)	C	3919 (V)
Quercetin	302.24	1.63	5	7	GB (0.55)	HIA (+)	AMES (+)	C	159 (III)
Apigenin	270.24	1.89	3	5	GB (0.55)	HIA (+)	AMES (−)	NC	2500 (V)
Morin	302.24	1.47	5	7	GB (0.55)	HIA (+)	AMES (−)	NC	3919 (V)
Chlorogenic acid	354.31	0.87	6	9	NGB (0.11)	HIA (+)	AMES (−)	NC	5000 (V)
Resveratrol	228.24	1.71	3	3	GB (0.55)	HIA (+)	AMES (−)	NC	1560 (IV)
Kaempferol	286.24	1.7	4	6	GB (0.55)	HIA (+)	AMES (−)	NC	3919 (V)
(+)-Catechin	290.27	1.33	5	6	GB (0.55)	HIA (+)	AMES (−)	NC	10000 (VI)
Isorhamnetin	316.26	2.35	4	7	GB (0.55)	HIA (+)	AMES (−)	NC	5000 (V)
(−)-Epicatechin	290.27	1.47	5	6	GB (0.55)	HIA (+)	AMES (−)	NC	10000 (VI)
(−)-Epigallocatechin gallate	458.37	1.53	8	11	NGB (0.17)	HIA (+)	AMES (−)	NC	1000 (IV)

a = molecular weight, b = octanol water partition coefficient, c = hydrogen bond donor, d = hydrogen acceptor donor, GB = good bioavailability, NGB = not good bioavailability, NC = non carciogenicity, C = Carciogenicity

3.3. Visual analysis of receptor-ligand complex interactions

The visual analysis aims to observe the interactions between the ligands (several test ligands were taken as samples and commercial ligands) as inhibitors and the amino acids of the target protein. Based on the 2D and 3D visualization results (Figures 4 and 5), interactions occurred at the catalytic active site residues in the form of hydrogen bond interactions on the amino acid residue.

These interactions occurred between Thr1011 in the XDH-Allopurinol and XDH-Apigenin complex (Figure 4A and 4D), Asn243 and Glu201 in the PNP-Ulodesine complex (Figure 4B), Asp330 in the GDA-Azepinomycin complex (Figure 4C), Tyr88 and Glu201 to the PNP-Morin complex (Figure 4E), His17 and Asp19 to the ADA-EHNA complex (Figure 4G), Glu217, Asp296, and Asp19 to the ADA-Catechin complex (Figure 4H).

Hydrophobic interactions occurred in the amino acid residues Arg881 and Phe915 on the XDH-Allopurinol and XDH-Apigenin complex (Figure 4A and 4D), Met219 on the PNP-Ulodesine and the PNP-Morin complex (Figure 4B and 4E). Other hydrophobic interactions occurred in Glu1261 and Val803 in the XDH-Apigenin complex (Figure 4D), Asn243 on the PNP-Morin complex (Figure 4E), Trp102 and Leu103 in the GDA-Azepinomycin complex (Figure 4C), Gly184, Glu217, and Asp296 in the ADA-EHNA complex (Figure 2G), Gly184 and His17 in the ADA-Catechin complex (Figure 4H). The protein catalytic active site residues are involved in the binding of purine substrates in the mechanism of uric acid formation [39]. The position of the interacting ligand on the active catalytic site of the receptor causes the receptor activity to be inhibited so that the receptor does not bind to the substrate and cannot form a product (uric acid) [24]. The interaction of the ligand-receptor complex can be seen in Table 7.
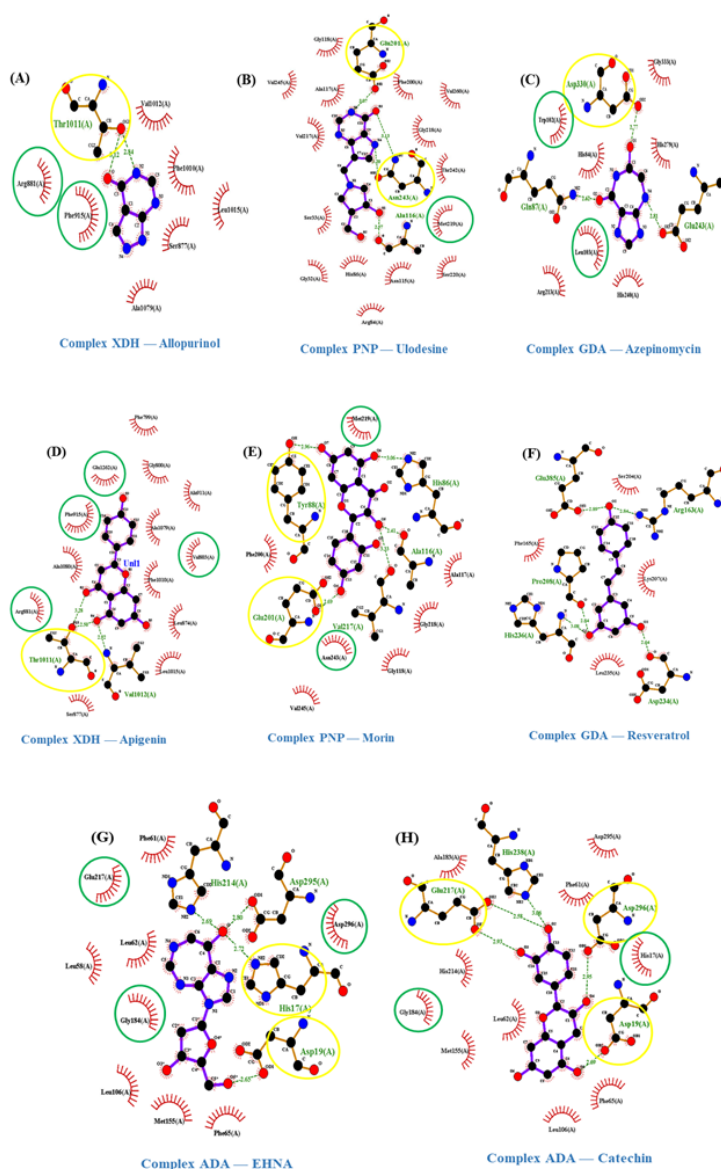

Figure 4. 2D visualization of the interaction of the target receptor complex with the test ligand (Notes: yellow circle = hydrogen bond interaction on the catalytic side, green circle = hydrophobic interaction on the catalytic side, dashed line = hydrogen bond interaction, ⌇⌇⌇ = non-ligand residues involved in hydrophobic bond)
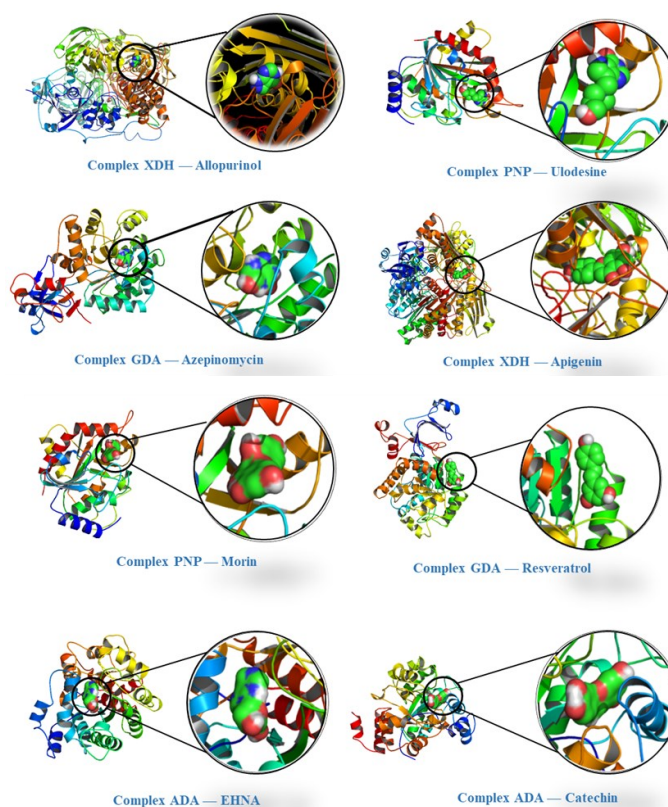
Figure 5. 3D visualization of the interaction between test ligand–target receptor complex

Table 7. Ligand–receptor complex interactions

Complex ligand-receptors	Energy affinity (kcal/mol)	Interacting residue	
		Hydrogen bond	Hydrophobic interactions
XDH–Allopurinol	–5.00	**Thr1011**	**Arg881**, Val1012, Phe1010, Leu1015, Ser877, Ala1079, **Phe915**
PNP–Ulodesine	–6.24	Ala116, **Asn243**, **Glu201**	Arg84, Asn115, Ser220, **Met219**, Thr242, Gly218, Val260, Phe200, Gly118, Ala117, Val245, Val217, Ser33, Gly32
GDA–Azepinomycin	–5.39	**Asp330**, Gln87, Glu243	**Trp102**, His54, Gly333, His279, His240, **Leu103**, Arg213
ADA–EHNA	–5.65	Asp181, Asp295, **His17**, **Asp19**	**Gly184**, Phe65, **Glu217**, Leu62, Met155, Leu106, **Asp296**, Phe61, Leu58
XDH–Apigenin	–8.28	**Thr1011**, Val1012	Phe799, **Glu1262**, Glu800, Ala911, Ala1079, **Val803**, Phe1010, Leu874, Leu1015, Ser877, **Arg88**, Ala1080, **Phe915**
PNP–Morin	–6.85	**Tyr88**, His86, Ala116, Val217, **Glu201**	**Met219**, Ala117, Gly218, Gly118, **Asn243**, Val245, Phe200
GDA–Resveratrol	–6.27	His236, Pro208, Asp234, Arg163, Glu385	Phe165, Leu235, Lys207, Ser204
ADA–Catechin	–7.73	**Glu217**, **Asp296**, His238, Asp19	**Gly184**, His214, Met155, Leu62, Leu106, **His17**, Asp295, Phe61, Ala183

The text in bold is the residue of the active catalytic site

4. Conclusion

According to molecular docking results, several compounds from the phenolic and flavonoid groups in garlic and black garlic are potential candidates for multi-target antigout therapy. Apigenin and isorhamnetin are the best compounds because they have significantly higher negative energy affinity values in all target receptors (XDH, GDA, PNP, NT5C2-1497, and NT5C2-1498) and have good scores in all Lipinski and ADMET parameters. Other compounds that have been proposed include (–)-epicatechin, (+)-catechin, kaempferol, and morin, which can inhibit five target receptors and have high scores in all Lipinski and ADMET parameters. Based on the visualization, the (+)-catechin and morin compounds bind exactly to the active catalytic site to inhibit the product's formation in the form of uric acid. These compounds should be clinically tested against inhibitors at each target receptor.

References

[1] Kazuki Abe, Yoji Hori, Takao Myoda, Volatile compounds of fresh and processed garlic (Review), *Experimental and Therapeutic Medicine*, 19, 2, (2020), 1585-1593 https://doi.org/10.3892/etm.2019.8394

[2] Jan Borlinghaus, Frank Albrecht, Martin C. H. Gruhlke, Ifeanyi D. Nwachukwu, Alan J. Slusarenko, Allicin: chemistry and biological properties, *Molecules*, 19, 8, (2014), 12591-12618 https://doi.org/10.3390/molecules190812591

[3] Shuxia Chen, Xiaoqing Shen, Siqiong Cheng, Panpan Li, Junna Du, Yanxia Chang, Huanwen Meng, Evaluation of garlic cultivars for polyphenolic content and antioxidant properties, *PLoS ONE*, 8, 11,

(2013), e79730
https://doi.org/10.1371/journal.pone.0079730

[4] Leyla Bayan, Peir Hossain Koulivand, Ali Gorji, Garlic: a review of potential therapeutic effects, *Avicenna Journal of Phytomedicine*, 4, 1, (2014), 1-14 https://dx.doi.org/10.22038/ajp.2014.1741

[5] Victor Manuel Beato, Francisco Orgaz, Francisco Mansilla, Alfredo Montaño, Changes in phenolic compounds in garlic (*Allium sativum* L.) owing to the cultivar and location of growth, *Plant Foods for Human Nutrition*, 66, 3, (2011), 218-223 https://doi.org/10.1007/s11130-011-0236-2

[6] Shunsuke Kimura, Yen-Chen Tung, Min-Hsiung Pan, Nan-Wei Su, Ying-Jang Lai, Kuan-Chen Cheng, Black garlic: A critical review of its production, bioactivity, and application, *Journal of Food and Drug Analysis*, 25, 1, (2017), 62-70 https://doi.org/10.1016/j.jfda.2016.11.003

[7] Il Sook Choi, Han Sam Cha, Young Soon Lee, Physicochemical and antioxidant properties of black garlic, *Molecules*, 19, 10, (2014), 16811-16823 https://doi.org/10.3390/molecules191016811

[8] S. M. Ammelia, R. Retnosari, Y. Utomo, D. Sukarianingsih, S. Wonorahardjo, The changing profiles of organosulfuric compounds during black garlic processing, *IOP Conference Series: Earth and Environmental Science*, 2020 https://doi.org/10.1088/1755-1315/475/1/012037

[9] Park Cheol, Park Sejin, Chung Yoon Ho, Kim Gi-Young, Choi Young Whan, Kim Byung Woo, Choi Yung Hyun, Induction of apoptosis by a hexane extract of aged black garlic in the human leukemic U937 cells, *Nutrition Research and Practice*, 8, 2, (2014), 132-137 https://doi.org/10.4162/nrp.2014.8.2.132

[10] Ozan Emre Eyupoglu, Antioxidant activities, phenolic contents and electronic nose analysis of black garlic, *International Journal of Secondary Metabolite*, 6, 2, (2019), 154-161 https://doi.org/10.21448/ijsm.564813

[11] Abdul Aziz Setiawan, Shirly Kumala, L. Dian Ratih, Nancy Dewi Yuliana, *In silico* study on s-allyl cysteine and quercetin from garlic (*Allium sativum* Linn) as xanthine oxidase inhibitor, *International Seminar on Pharmaceutical Sciences and Technology*, (2019), 1-7

[12] Maria Giulia Battelli, Letizia Polito, Massimo Bortolotti, Andrea Bolognesi, Xanthine oxidoreductase in drug metabolism: beyond a role as a detoxifying enzyme, *Current Medicinal Chemistry*, 23, 35, (2016), 4027-4036 http://dx.doi.org/10.2174/0929867323666160725091915

[13] Durga Mahor, Gandham S. Prasad, Biochemical characterization of *Kluyveromyces lactis* adenine deaminase and guanine deaminase and their potential application in lowering purine content in beer, *Frontiers in Bioengineering and Biotechnology*, 6, 180, (2018), 1-11 https://doi.org/10.3389/fbioe.2018.00180

[14] Durga Mahor, Anu Priyanka, Gandham S. Prasad, Krishan Gopal Thakur, Functional and structural characterization of purine nucleoside phosphorylase from *Kluyveromyces lactis* and its potential applications in reducing purine content in food, *PLoS*

ONE, 11, 10, (2016), e0164279 https://doi.org/10.1371/journal.pone.0164279

[15] Linmeng Tang, Dehong Yang, Yaohui Wang, Xu Yang, Kai Chen, Xingyu Luo, Jun Xu, Yujia Liu, Zheng Tang, Qianqian Zhang, 5′-Nucleotidase Plays a Key Role in Uric Acid Metabolism of *Bombyx mori*, *Cells*, 10, 9, (2021), 2243 https://doi.org/10.3390/cells10092243

[16] A.-K. Tausche, M. Christoph, M. Forkmann, U. Richter, S. Kopprasch, C. Bielitz, M. Aringer, C. Wunderlich, As compared to allopurinol, urate-lowering therapy with febuxostat has superior effects on oxidative stress and pulse wave velocity in patients with severe chronic tophaceous gout, *Rheumatology International*, 34, 1, (2014), 101-109 https://doi.org/10.1007/s00296-013-2857-2

[17] Thomas Bardin, Pascal Richette, Impact of comorbidities on gout and hyperuricaemia: an update on prevalence and treatment options, *BMC Medicine*, 15, 123, (2017), 1-10 https://doi.org/10.1186/s12916-017-0890-9

[18] Preethi Johnson, Chitra Loganathan, Ancy Iruthayaraj, Kumaradhas Poomani, Palvannan Thayumanavan, S-allyl cysteine as potent anti-gout drug: insight into the xanthine oxidase inhibition and anti-inflammatory activity, *Biochimie*, 154, (2018), 1-9 https://doi.org/10.1016/j.biochi.2018.07.015

[19] Cen Zhang, Rui Wang, Guowen Zhang, Deming Gong, Mechanistic insights into the inhibition of quercetin on xanthine oxidase, *International Journal of Biological Macromolecules*, 112, (2018), 405-412 https://doi.org/10.1016/j.ijbiomac.2018.01.190

[20] Douglas B. Kitchen, Hélène Decornez, John R. Furr, Jürgen Bajorath, Docking and scoring in virtual screening for drug discovery: methods and applications, *Nature Reviews Drug discovery*, 3, 11, (2004), 935-949 https://doi.org/10.1038/nrd1549

[21] Ji-Sang Kim, Ok-Ju Kang, Oh-Cheon Gweon, Comparison of phenolic acids and flavonoids in black garlic at different thermal processing steps, *Journal of Functional Foods*, 5, 1, (2013), 80-86 https://doi.org/10.1016/j.jff.2012.08.006

[22] Zhichang Qiu, Zhenjia Zheng, Bin Zhang, Dongxiao Sun-Waterhouse, Xuguang Qiao, Formation, nutritional value, and enhancement of characteristic components in black garlic: A review for maximizing the goodness to humans, *Comprehensive Reviews in Food Science and Food Safety*, 19, 2, (2020), 801-834 https://doi.org/10.1111/1541-4337.12529

[23] Katarzyna Najman, Anna Sadowska, Ewelina Hallmann, Influence of thermal processing on the bioactive, antioxidant, and physicochemical properties of conventional and organic agriculture black garlic (*Allium sativum* L.), *Applied Sciences*, 10, 23, (2020), 8638 https://doi.org/10.3390/app10238638

[24] Edmond Joseph Pierre Lommen, Hypoxanthine-guanine phosphoribosyltransferase deficiency: a clinical and biochemical study, Paediatric Department, Radboud University Nijmegen, Netherlands, 1973

[25] Rakhi Seth, Alison S. R. Kydd, Rachelle Buchbinder, Claire Bombardier, Christopher J. Edwards, Allopurinol for chronic gout, *Cochrane Database of*

Systematic Reviews, 10, (2014), 1-75 https://doi.org/10.1002/14651858.CD006077.pub3

[26] Ravi K. Ujjinamatada, Anila Bhan, Ramachandra S. Hosmane, Design of inhibitors against guanase: synthesis and biochemical evaluation of analogues of azepinomycin, *Bioorganic & Medicinal Chemistry Letters*, 16, 21, (2006), 5551-5554 https://doi.org/10.1016/j.bmcl.2006.08.033

[27] Sebastian E. Sattui, Angelo L. Gaffo, Treatment of hyperuricemia in gout: current therapeutic options, latest developments and clinical implications, *Therapeutic Advances in Musculoskeletal Disease*, 8, 4, (2016), 145-159 https://doi.org/10.1177%2F1759720X16646703

[28] Federico Cividini, Rossana Pesi, Laurent Chaloin, Simone Allegrini, Marcella Camici, Emeline Cros-Perrial, Charles Dumontet, Lars Petter Jordheim, Maria Grazia Tozzi, The purine analog fludarabine acts as a cytosolic 5′-nucleotidase II inhibitor, *Biochemical Pharmacology*, 94, 2, (2015), 63-68 https://doi.org/10.1016/j.bcp.2015.01.010

[29] Barbara Kutryb-Zajac, Paulina Mierzejewska, Ewa M. Slominska, Ryszard T. Smolenski, Therapeutic perspectives of adenosine deaminase inhibition in cardiovascular diseases, *Molecules*, 25, 20, (2020), 4652 https://doi.org/10.3390/molecules25204652

[30] Oleg Trott, Arthur J. Olson, AutoDock Vina: improving the speed and accuracy of docking with a new scoring function, efficient optimization, and multithreading, *Journal of Computational Chemistry*, 31, 2, (2010), 455-461 https://doi.org/10.1002/jcc.21334

[31] David Ramírez, Julio Caballero, Is it reliable to take the molecular docking top scoring position as the best solution without considering available structural data?, *Molecules*, 23, 5, (2018), 1038 https://doi.org/10.3390/molecules23051038

[32] Eric W. Bell, Yang Zhang, DockRMSD: an open-source tool for atom mapping and RMSD calculation of symmetric molecules through graph isomorphism, *Journal of Cheminformatics*, 11, 40, (2019), 1-9 https://doi.org/10.1186/s13321-019-0362-7

[33] Xing Du, Yi Li, Yuan-Ling Xia, Shi-Meng Ai, Jing Liang, Peng Sang, Xing-Lai Ji, Shu-Qun Liu, Insights into protein–ligand interactions: mechanisms, models, and methods, *International Journal of Molecular Sciences*, 17, 2, (2016), 144 https://doi.org/10.3390/ijms17020144

[34] Nguyen Thanh Nguyen, Trung Hai Nguyen, T. Ngoc Han Pham, Nguyen Truong Huy, Mai Van Bay, Minh Quan Pham, Pham Cam Nam, Van V. Vu, Son Tung Ngo, Autodock vina adopts more accurate binding poses but autodock4 forms better binding affinity, *Journal of Chemical Information and Modeling*, 60, 1, (2020), 204-211 https://doi.org/10.1021/acs.jcim.9b00778

[35] Young Bin Choy, Mark R. Prausnitz, The rule of five for non-oral routes of drug delivery: ophthalmic, inhalation and transdermal, *Pharmaceutical Research*, 28, 5, (2011), 943-948 https://doi.org/10.1007/s11095-010-0292-6

[36] Shelly Pathania, Pankaj Kumar Singh, Analyzing FDA-approved drugs for compliance of pharmacokinetic principles: should there be a critical screening parameter in drug designing protocols?, *Expert Opinion on Drug Metabolism & Toxicology*, 17, 4, (2021), 351-354 https://doi.org/10.1080/17425255.2021.1865309

[37] Feixiong Cheng, Weihua Li, Yadi Zhou, Jie Shen, Zengrui Wu, Guixia Liu, Philip W. Lee, Yun Tang, admetSAR: a comprehensive source and free tool for assessment of chemical ADMET properties, *Journal of Chemical Information and Modeling*, 52, 11, (2012), 3099–3105 https://doi.org/10.1021/ci300367a

[38] Longfei Guan, Hongbin Yang, Yingchun Cai, Lixia Sun, Peiwen Di, Weihua Li, Guixia Liu, Yun Tang, ADMET-score–a comprehensive scoring function for evaluation of chemical drug-likeness, *MedChemComm*, 10, 1, (2019), 148-157 https://doi.org/10.1039/C8MD00472B

[39] Hongnan Cao, James M. Pauff, Russ Hille, X-ray crystal structure of a xanthine oxidase complex with the flavonoid inhibitor quercetin, *Journal of Natural Products*, 77, 7, (2014), 1693-1699 https://doi.org/10.1021/np500320g